Optical and transport properties of NbN thin films revisited

S. Kern[1*], P. Neilinger[1, 2], M. Poláčková[1], M. Baránek[1], T. Plecenik[1], T. Roch[1], and M. Grajcar[1, 2]

[1]Department of Experimental Physics, Comenius University, SK-84248 Bratislava, Slovakia

[2]Institute of Physics, Slovak Academy of Sciences, Dúbravská cesta, Bratislava, Slovakia

*samuel.kern@fmph.uniba.sk

Introduction & Abstract

Highly disordered NbN thin films exhibit promising superconducting and optical properties. Despite extensive study, discrepancies in its basic electronic properties persist. Analysis of the optical conductivity of disordered ultra-thin NbN films, obtained from spectroscopic ellipsometry by standard Drude-Lorentz model, provides inconsistent parameters. We argue that this discrepancy arise from neglecting the presence of quantum corrections to conductivity in the IR range. To resolve this matter, we propose a modification to the Drude-Lorentz model, incorporating quantum corrections. The parameters obtained from the modified model are consistent not only with transport and superconducting measurements but also with ab initio calculations. The revisited values describing conduction electrons, which differ significantly from commonly adopted ones, are the electron relaxation rate $\Gamma \approx 1.8$ eV/ħ, the Fermi velocity $v_F \approx 0.7 \times 106$ ms^{-1} and the electron density of states $N(E_F) = 2$ states of both spins/eV/NbN.

Common approach to opical properties of NbN

- Drude-Lorentz model
  - scattering rate $\Gamma \sim 0.3$ eV [1,2] (typical for clean metals)
  - two Lorentz oscillators (at 1 eV and 6 eV) describing interband transitions
- The interband transitions largely supported by JDOS from ab-inio simulations (see Fig. 1) [3]

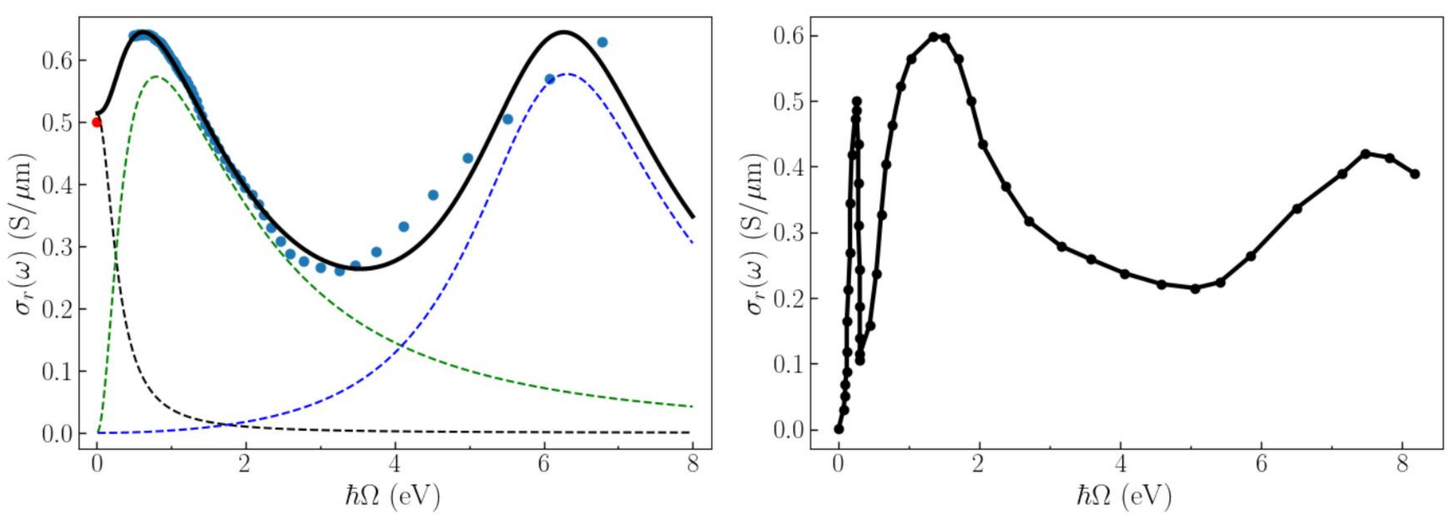

Fig. 1 Left: real part of optical conductivity of NbN obtained from SE measurement (blue dots) and fitted to Drude-Lorentz model (black solid line) with individual contributions shown as dashed lines [1]. Right: Real part of optical conductivity given by JDOS obtained from DFT simulations [3].

- The parameters produce inconsistent picture of conducting electrons!

$\boxed{n = \sigma_0 m_e \Gamma / e^2 \sim 10^{27}\,\mathrm{m}^{-3}}$ $\boxed{v_F = l\Gamma \sim 10^4\ \mathrm{m/s}}$

Quantum corrections to optical conductivity

- NbN - highly disordered metal approaching MIT [1]
  - Highly disordered metals exhibit

$$k_F l \sim 1$$

  - alternativelly

$$\hbar\Gamma \sim E_F$$

- Thus, the relaxation rate Γ of highly disordered metals is [4]

$$\boxed{\hbar\Gamma \sim 1\ \mathrm{eV}}$$

- For $\omega < \Gamma$ the real part of optical conductivity σ_r exhibits square-root corrections, (which should dissapear at Γ [4,5])

$$\frac{\delta\sigma_r}{\sigma_0} \propto -\sqrt{\omega}$$

- NbN can not be analysed as ordinary (clean) metal with $\hbar\Gamma \sim 0.1$ eV!
- High Γ and the squre-root corrections affects the plasma frequency and create new frequency where $\varepsilon_r = 0$ (double epsilon-near-zero [6])

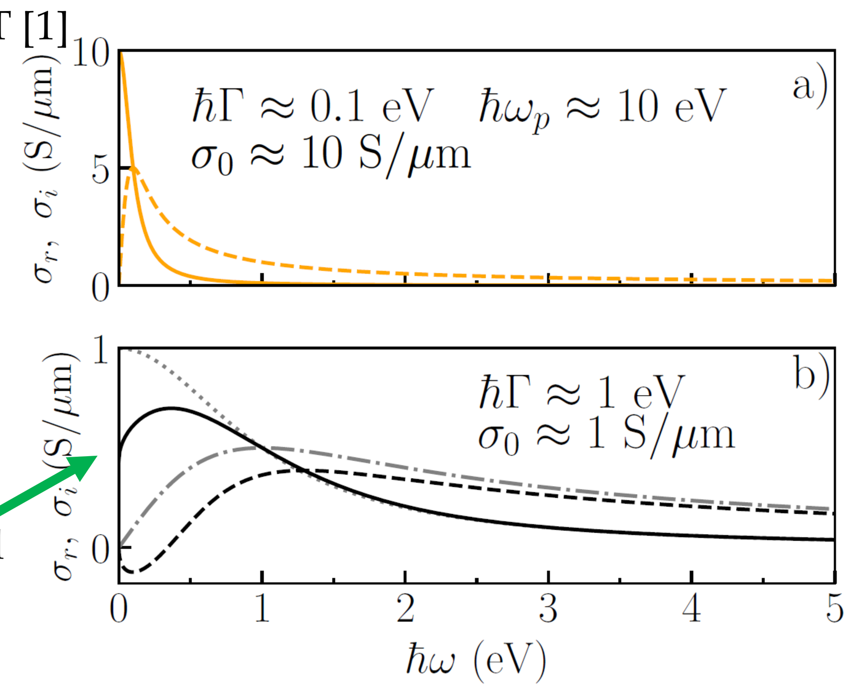

Fig. 2: a) optical conductivity of a clean metal as described by the Drude model ($\Gamma \approx 0.1$ eV). Clean metals exhibit $\varepsilon_r = 0$ at the plasma frequency ω_p. b) optical conductivity of disordered metal – exhibits high scattering rate $\Gamma \approx 1$ eV and the square-root corrections. Plasma frequency is shifted and another plasma frequency appears!

Model for optical properties of thin NbN films

- Quantum corrections to optical conductivity due to the disorder and the el-el interaction effects – alternative picture for the IR spectra in NbN.
- Large $\hbar\Gamma \sim 1$ eV smears the bandstructure (confirmed in ARPES results [7]) → the 1 eV interband transition disappears.
- The peaks is the fade out of the square root quantum corrections.
- NbN optical conductivity from SE was analyzed by the quantumn-corrected Drude Lorentz model (see Fig. 3)

$$\sigma_r(\omega) = \frac{\sigma_0}{1+(\omega/\Gamma)^2}\left(1 - Q^2\left(1-\sqrt{\omega/\Gamma}\right)e^{-2(\omega/\Gamma)^2}\right) + \frac{\sigma_1(\omega\Gamma_1)^2}{(\omega\Gamma_1)^2 + (\omega_1^2-\omega^2)^2} \quad (1)$$

$$\sigma_i(\omega) = \mathcal{H}[\sigma_r(\omega)] - (\varepsilon_\infty - 1)\varepsilon_0\omega$$

- Obtained relaxation rate: $\hbar\Gamma \sim 1.8$ eV.
- Interband transition at 5 - 7 eV matches the simulations [3].
- $\hbar\Gamma \sim 2$ eV predicted also from bandsrtucture-smearing necessary to stabilize the crystaline structure in DFT [8].

Results

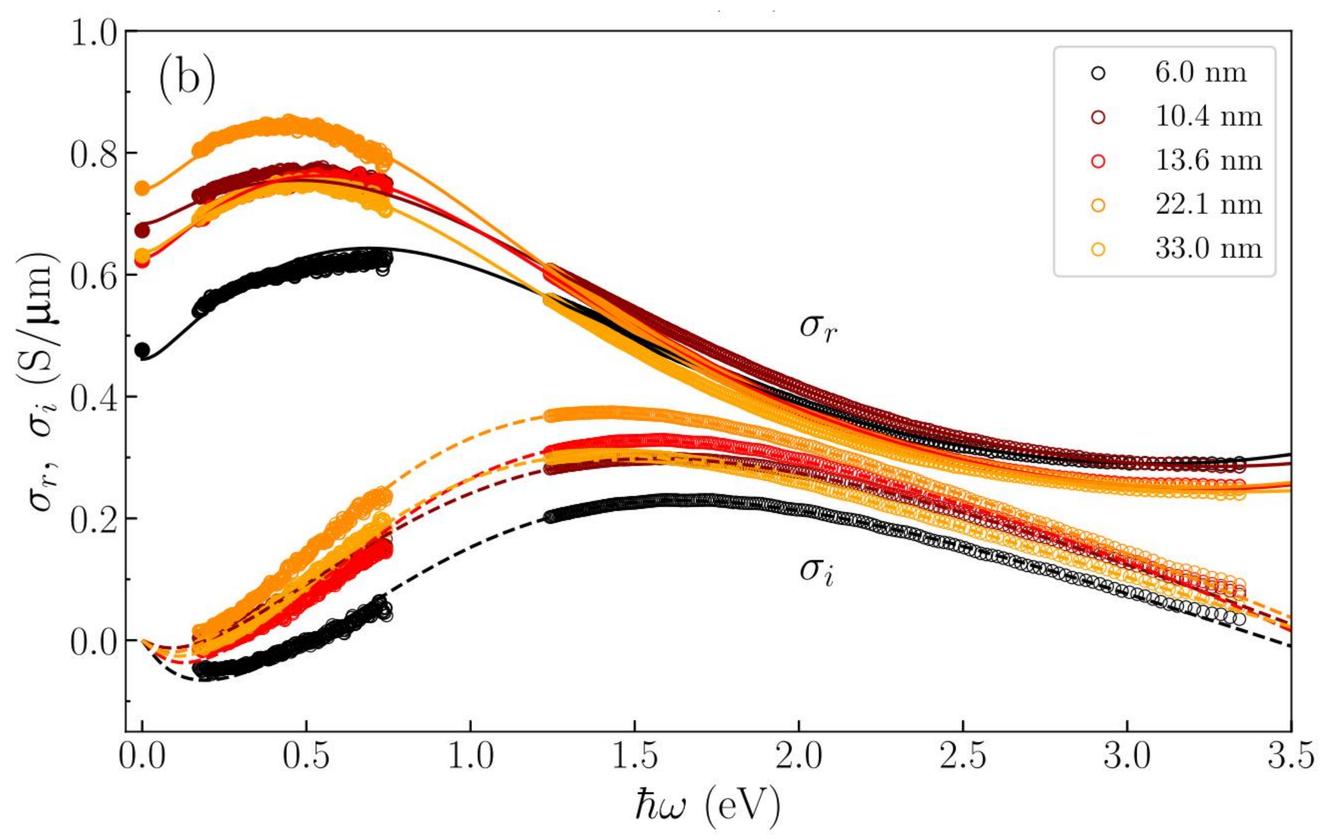

Fig. 3 Thick lines: real and imaginary part of optical conductivity for NbN films of various thickness, determined by SE. Thin lines are fitted to Eq. (1). Data at $\omega = 0$: room-temperature DC conductivities measured by van der Pauw method.

The real part of $\varepsilon(\omega)$ is zero at two frequencies belov the UV range

The ordinary plasma frequency $\hbar\omega_p \approx 3$ eV

Second „plasma" frequency ω_{p2} explained by quantum corrections $\omega_{p2} \approx \Gamma Q^4$

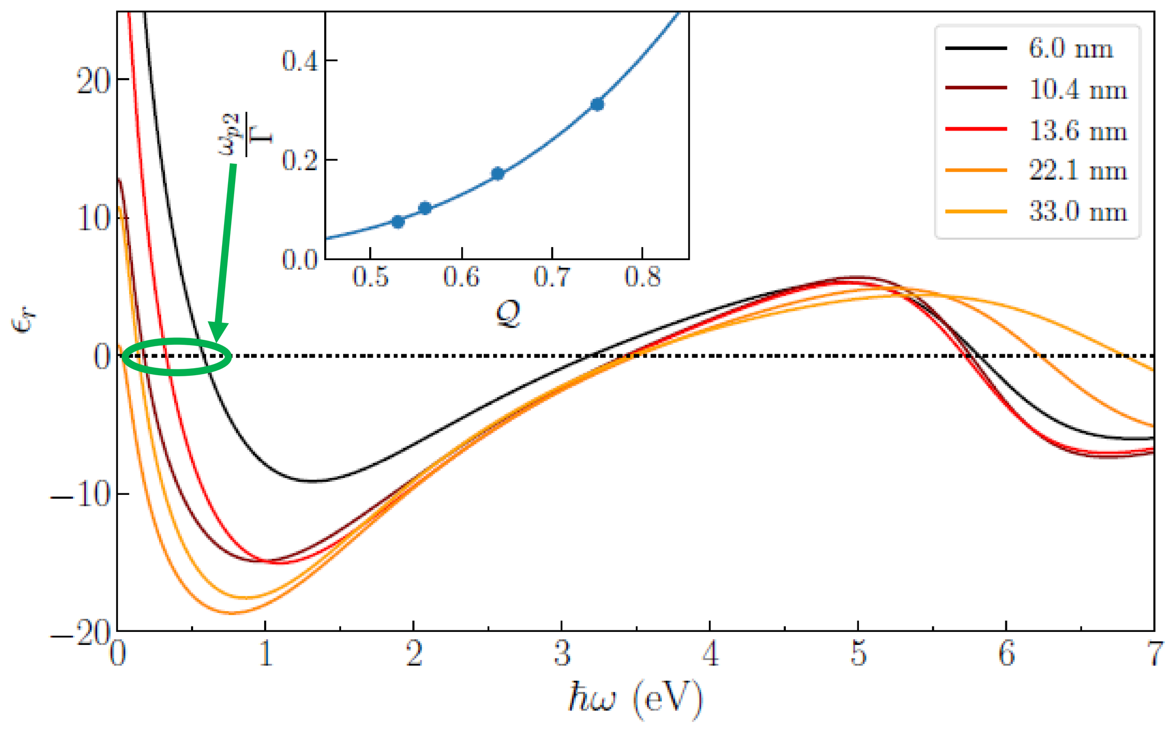

Fig. 4 The real part of the dielectric function $\varepsilon(\omega)$ corresponding to the conductivities in Fig. 3. The inset shows the lower plasma frequencies (frequencies at which $\varepsilon(\omega) = 0$) dependent on quantumness Q.

Magnetoresistance at low temperatures was measured yealding $B_{c2}(T)$ curves.

- Estimated diffusivity $D_{B_{c2}}$ is comparable to the difusivity calculated from the optical model D_{opt} (see Table. 1).
- Opposite trend of the thickness dependance of $D_{B_{c2}}$!.

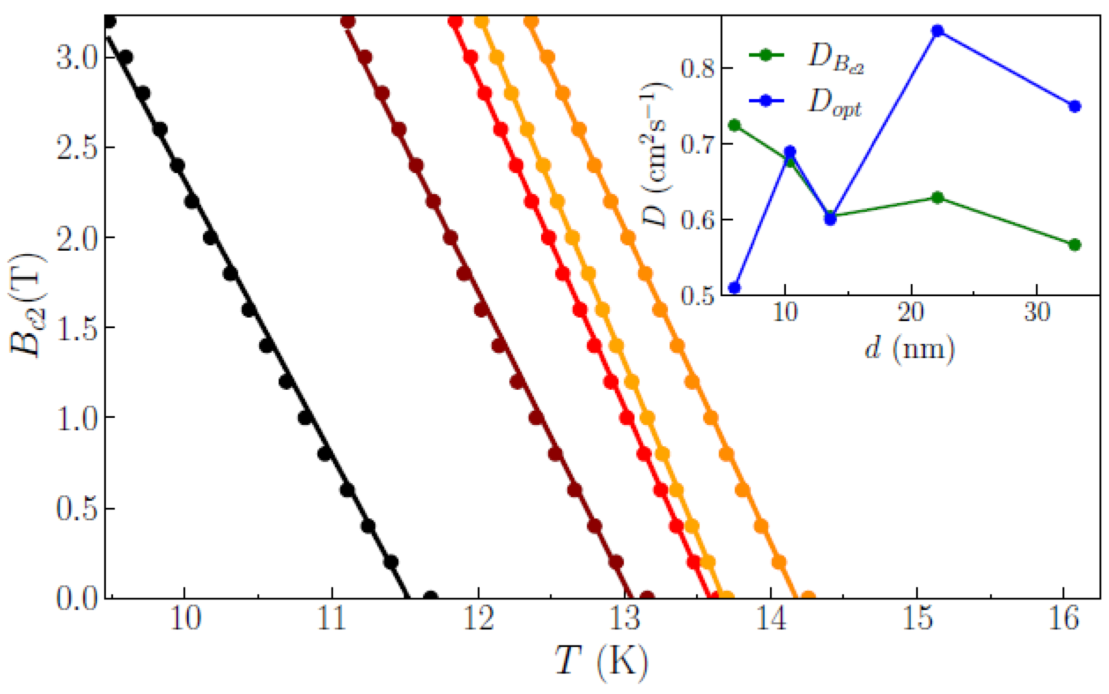

Fig. 5 The solid lines are linear fits to the $B_{c2}(T)$ data (dots). The color-coding is same as in Fig. 3. The inset shows a comparison of the diffusivity obtained from the slope of B_{c2} (green) and that estimated from the proposed optical model D_{opt} (blue).

d (nm)	$k_F l$ (1) $1/Q$	D_{opt} (cm² s^{-1}) $\frac{\hbar}{3Qm_e}$	$D_{B_{c2}}$ (cm² s^{-1}) $-\frac{4k_B}{\pi e}\left(\frac{\partial B_{c2}}{\partial T}\right)^{-1}_{T_c}$	v_F (10^6 ms^{-1}) $\sqrt{\frac{\hbar\Gamma}{Qm_e}}$	n (10^{28} m^{-3}) $\frac{\sigma_0\Gamma m_e}{e^2}$
6.0	1.33	0.51	0.73	0.66	8.82
10.4	1.78	0.69	0.68	0.77	9.57
13.6	1.56	0.60	0.60	0.70	9.80
22.1	2.22	0.86	0.63	0.85	9.42
33.0	1.88	0.73	0.57	0.76	8.86

Table 1: Comparison of diffusivities obtained from optical and magnetoresistance measurements. Estimated Fermi velocity and density of carriers.

References

[1] A. Semenov, et al., Phys. Rev. B 80, 054510 (2009)
[2] N. D. Kuz'michev and G. P. Motulevich, Zh. Eksp. Teor. Fiz. 84, 2316 (1983).
[3] J. Pflüger, et al., Phys. Rev. B 31, 1244 (1985).
[4] P. Neilinger, et al., Phys. Rev. B 100, 241106(R) (2019).
[5] B. Altshuler and A. Aronov, edited by A. Efros and M. Pollak (North Holland, 1985).
[6] Y. Ran, H. Lu, S. Zhao, Q. Guo, C. Gao, Z. Jiang, and Z. Wang, Applied Surface Science 537, 147981 (2021).
[7] T. Yu, et al., Science Advances 7, eabi5833 (2021).
[8] K. R. Babu and G.-Y. Guo, Physical Review B 99, 104508 (2019).

Acknowledgements

Funded by the European Union

RECOVERY AND RESILIENCE PLAN

MINISTRY OF INVESTMENTS, REGIONAL DEVELOPMENT AND INFORMATIZATION OF THE SLOVAK REPUBLIC

This work was supported by the project skQCI No. (101091548), founded by the European Union (DIGITAL) and the Recovery and Resilience Plan of the Slovak Republic and the Operational Program Integrated Infrastructure for the projects: Advancing University Capacity and Competence in Research, Development and Innovation (ACCORD, ITMS2014 + :313021X329)